

**EXPERIMENTAL EVALUATION OF THE SYNTHETIC SOLID ELECTROLYTE INTERFACE (SSEI) CONCEPT FOR THE PRIMARY Ca-SOCl<sub>2</sub> BATTERY SYSTEM**

Prepared by:

Dr. J. P. de Neufville

Voltaix, Inc., P.O. Box 5357, 197 Meister Ave. North Branch, NJ 08876

December 1988

Final Report under Contract DAAL 01-88-C-0820  
for Period 15 April 1988 to 15 October 1988DTIC  
ELECT  
MAY 11 1990  
S B D**Project Summary:**

The Ca-SOCl<sub>2</sub> primary battery system has an excellent safety profile when subjected to a variety of abuse test conditions. Furthermore its theoretical energy density qualifies it for a variety of demanding Army and other DOD applications. Recently, significant improvements have been reported in the low temperature performance and the cathode capacity obtainable in this system. One major remaining flaw, however, is the corrosion of the Ca anode during storage at elevated temperature. Efforts to modify the electrolyte or provide a protective coating for the anode have had only limited success. The purpose of the present research has been to apply the concept of a synthetic solid electrolyte interface (SSEI) to overcome the problem of Ca corrosion in Ca-SOCl<sub>2</sub> primary cells.

To this end, coatings based on the Ca-Ge-S system were RF sputter-coated onto scraped Ca anodes and cells with these coated anodes were stored and discharged at 6.5mA/cm<sup>2</sup> at 21°C. The morphology and surface composition of the coated anodes, both as deposited and after partial discharge, were determined using Scanning Electron Microscopy (SEM) and Energy Dispersive X-ray Spectroscopy (EDS). Based on the consistent observation of a small additional cell polarization (about 0.05 - 0.3V at 6.5mA/cm<sup>2</sup>) for the coated anode cells, and the SEM/EDS evidence that the coating was able, in most cases, to remain intact during partial discharge, we were able to conclude that these Ca-Ge-S coatings, particularly when modified or "doped" with small (up to 4%) concentrations of Sr and Y, are Ca<sup>++</sup> ion conductors with ionic conductivities in the range of 10<sup>-7</sup> to 10<sup>-5</sup> ohm<sup>-1</sup> cm<sup>-1</sup>. Furthermore, since the coatings were insoluble in the Ca(AlCl<sub>4</sub>)<sub>2</sub>-SOCl<sub>2</sub> catholyte, they can function as the sought after SSEI under these conditions.

If these observations can be successfully extended to higher storage temperatures, lower operating temperatures, and high rate wound cell configurations, then the SSEI concept could make a major contribution to the implementation of the Ca-SOCl<sub>2</sub> battery technology for Army, other DOD and commercial applications. Achieving these objectives is the basis of a Phase II proposal.

**DISTRIBUTION STATEMENT A**Approved for public release;  
Distribution Unlimited

00 05 10 030

AD-A221 872

Section	TABLE OF CONTENTS	Page
1. Introduction		5
2. Deposition of Coatings		7
2.1 Experimental		7
2.1.1 Binary Films		8
2.1.2 Ternary Films		9
2.1.3 Quaternary and Quinary Films		9
2.2 Results and Discussion		9
2.2.1 Thickness and Composition		9
2.2.2 Morphology and Ca Passivation		11
2.3 Conclusions		17
3. Testing of Beaker Cells		17
3.1 Experimental		17
3.2 Results and Discussion		19
3.2.1 Electrochemical Testing		19
3.2.2 Anode Morphology and Surface Chemistry (SEM & EDS)		27
3.3 Conclusions		32
4. Summary		32
5. References		34



STATEMENT "A" per Charles Walker  
 AMC LABCOM Electronics Technology &  
 Devices Laboratory/SLCET-PR  
 Ft. Monmouth, NJ 07703  
 TELECON 5/10/90

VG

Accession For	
NTIS GRA&I	<input checked="" type="checkbox"/>
DTIC TAB	<input type="checkbox"/>
Unannounced	<input type="checkbox"/>
Justification	
By <i>per telecon</i>	
Distribution/	
Availability Codes	
Dist	Avail and/or Special
<i>A-1</i>	

## LIST OF ILLUSTRATIONS

Figure		Page
1.	Sample #1, SEM micrograph of Uncoated Calcium, 1000X.	12
2.	Sample #1, SEM micrograph of Uncoated Calcium, 5100X.	12
3.	Sample #2, SEM micrograph Ca-Ge-S film, 0.4 microns thick, 500X.	13
4.	Sample #2, SEM micrograph of Ca-Ge-S film, 0.4 microns thick, 5000X.	13
5.	Sample #19, SEM micrograph of Ca-Y-Ge-S film, 3.5 microns thick, 6000X, 43° tilt.	15
6.	Sample #19, SEM micrograph of Ca-Y-Ge-S film, 3.5 microns thick, 5000X, 83° tilt.	15
7.	Sample #6, SEM micrograph of Ca-Sr-Y-Ge-S film, 0.8 microns thick, 100X.	16
8.	Sample #6, SEM micrograph of Ca-Sr-Y-Ge-S film, 0.8 microns thick, 5000X.	16
9.	Discharge data for reference and ternary coated anodes.	20
10.	Discharge data for reference Ca in A.P.L. electrolyte.	23
11.	Discharge of a Ca-Sr-Ge-S coated anode vs. reference.	25
12.	Discharge of a Ca-Y-Ge-S coated anode vs. reference Ca.	26
13.	Sample #12, SEM micrograph of discharged calcium electrode, 100X.	29
14.	Sample #15, SEM micrograph of discharged Ca-Sr-Y-Ge-S coated electrode, 0.8 microns thick, 500X.	31
15.	Sample #16, SEM micrograph of discharged Ca-Sr-Y-Ge-S coated electrode, 2.2 microns thick, 500X.	31

# LIST OF TABLES

Table		Page
1.	Representative Coatings Thicknesses and Compositions.	10
2.	Ca <sup>++</sup> Ionic Conductivities of SSEI Coatings	27
3.	EDS Analysis of Discharged Electrodes	29

## 1. INTRODUCTION

The  $\text{Ca-SOCl}_2$  battery chemistry is an excellent candidate to provide safe operation in batteries significantly larger than 1kg operated at steady rates greater than the "C" rate in Army applications requiring high energy density batteries. Progress has already been reported<sup>1-3</sup> on optimizing the electrolyte composition and the cathode structure to minimize IR losses and maximize cathode capacity at relatively high specific rates (i.e., up to  $20 \text{ mA/cm}^2$ ). However, a serious problem of anode corrosion has been encountered in this system, particularly for cells stored at elevated temperature<sup>1,4-7</sup>. Since this corrosion appears to involve the formation of  $\text{CaCl}_2$ , an ionic compound with low ionic conductivity which is insoluble in the  $\text{Ca(AlCl}_4)_2\text{-SOCl}_2$  catholyte, it can be confidently anticipated that some degree of anode passivation, particularly at low temperature, will constitute an additional limitation on the performance of this cell chemistry at high discharge rates.

A further problem with the spontaneously formed insoluble  $\text{CaCl}_2$  corrosion product is that, not only is its ionic conductivity low, but it is anionic<sup>7</sup>. Thus, during discharge,  $\text{Cl}^-$  ions will migrate towards the positively charged anode, forming  $\text{CaCl}_2$  at the Ca interface. Concurrently, presumably, the newly formed  $\text{CaCl}_2$  is being dissolved at the catholyte- $\text{CaCl}_2$  interface by the excess  $\text{AlCl}_3$  left over from the creation of the  $\text{Cl}^-$  ions. Thus, in principle, the  $\text{CaCl}_2$  can function as an SEI (solid electrolyte

interface)<sup>1</sup>, but with a twist: instead of existing as a stable ionic membrane, as in the Li-SOCl<sub>2</sub> system, it must be constantly forming and redissolving at even the lowest discharge rates. Thus, such coatings are expected to behave poorly as inhibitors of Ca corrosion.

The primary goal in this Phase I study was to design and evaluate synthetic SEI,s (SSEI)<sup>8</sup> for Ca anodes by preparing RF sputtered coatings which are insoluble in the Ca(AlCl<sub>4</sub>)<sub>2</sub>-SOCl<sub>2</sub> catholyte and are cationic conductors for Ca<sup>+2</sup> ions. The compositions selected are based on the composition GeS<sub>2</sub>, which has an atomic structure generally similar to that of amorphous silica. It is also known to be an effective matrix for the solid-state ionic conduction of alkali metal ions. By analogy to the better understood silica-based alkali oxide systems, most of the strong, covalent Ge-S bonds are expected to be retained as alkaline earth sulfide species are added, with the added sulfide anions attaching themselves to (and locally terminating) that covalent network, and the alkaline earth ions dissolving "interstitially" within the network. Clearly this structure provides a good possibility for enhanced cationic conductivity (the Ge-S network being selected in preference to the Si-O network to provide a polarizable matrix for the highly charged Ca cations) with minimal anionic conductivity (the anions exist as large polymeric entities, possessing zero mobility). Such a coating has the possibility of functioning as an SSEI with the property that it could, in principle, retain its physical and chemical structure during discharge.

It should be pointed out that the present efforts to apply the SSEI concept to the control of Ca corrosion in Ca-SOCl<sub>2</sub> cells involved the exploration of many experimental variables in order to achieve an indication of the efficacy of the approach. In particular, the discovery of a usable coating and its preliminary optimization absorbed the majority of the Phase I effort. Thus this final report for Phase I emphasizes the history of that discovery and the evidence on which it is based. The important task of demonstrating that this development, documented so far only in beaker cells, has applicability in the high rate and high energy density cylindrical cells required for Army applications remains to be accomplished. This effort, which is continuing at Voltaix under an internally funded program, has as its limited objective the demonstration of Ca corrosion protection in wound cells stored at elevated temperature. Results of these studies will be reported to LABCOM as soon as they are available.

## 2. DEPOSITION OF COATINGS

### 2.1 Experimental

Coatings were sputter deposited on 3.2 cm<sup>2</sup> calcium metal coupons and previously weighed cover glass slips using a plasma generated in an atmosphere of 5% H<sub>2</sub>S in Ar and using targets of varying composition to achieve varying coating compositions. Sputtering power was maintained at 0.8 W/cm<sup>2</sup>, gas pressure was reproducibly fixed at 7 mTorr, and film thickness was varied by variation of the sputtering time. The film thicknesses were calculated based

on the weight gain of the coated cover slips and the assumed film density based on composition and the molar volume of the constituent species. Deposition rates ranged between 58 - 270 Å/min.

Coating structure, morphology and composition were determined using a scanning electron microscope (SEM) equipped with an energy dispersive X-ray spectrometer (EDS) for quantifying the intensity and spectral distribution of the electron beam induced characteristic X-rays. No matrix effects were considered in analyzing these data, so the results, obtained as relative peak intensities, though only semiquantitative, are nonetheless very useful for comparative purposes. The detection limit of this technique under the conditions utilized in these experiments is about 1%.

#### 2.1.1 Binary Films

The first films evaluated in this program were formed by sputtering a pure germanium target in an atmosphere of 5% H<sub>2</sub>S in Ar, using freshly scraped coupons of Ca metal as the substrate. Under these conditions the hydrogen sulfide molecules are partially dissociated and ionized, with neutral sulfur atoms, HS radicals and H<sub>2</sub>S molecules diffusing to both the substrate's and the target's exposed surfaces where they can react to form germanium sulfide. The germanium sulfide species on the target are, in turn, sputtered off and redeposited on the substrate. The net effect of these processes is to form a coating on the scraped Ca coupons with the approximate stoichiometry GeS<sub>2</sub>. In an attempt to

introduce  $\text{Ca}^{++}$  ions, the films were annealed for various periods of time at  $300^{\circ}\text{C}$ .

### 2.1.2 Ternary Films

In order to incorporate the  $\text{Ca}^{++}$  ions into the coating during its deposition, the sputtering target was modified by affixing coupons of Ca metal, presenting a composite surface to the incoming argon ions. The coatings so formed had the approximate stoichiometry  $\text{Ca}_{.33}\text{Ge}_{.33}\text{S}_{.33}$ .

### 2.1.3 Quaternary and Quinary Films

To explore the effects of additional alloying components on the coating structure, morphology and  $\text{Ca}^{++}$  ionic conductivity, exploratory coating studies were undertaken in which a small portion of the  $\text{Ca}^{++}$  ions were substituted by  $\text{Sr}^{++}$  or  $\text{Y}^{+3}$  ions, or by both simultaneously. Such coatings were prepared in the same fashion as the ternary coatings described above, except that additional coupons of Sr metal or Y metal or both were affixed onto the composite Ca + Ge cathode. The resultant coatings contained trace amounts of these additional elements, of order 4% in the case of Sr and less than 1% in the case of Y.

## 2.2 Results and Discussion

### 2.2.1 Coating Thickness and Composition

Representative coating thicknesses and compositions are listed in Table 1.

TABLE 1 - Representative Coating Thicknesses and Compositions.

Sam- ple #	Thickness, microns; (cation(s))	Relative EDS Signal				
		Ca	S	Ge	Sr	Y
1	(none)	1.0	-	-	-	-
2	0.44 (Ca)	0.34	0.37	0.30	-	-
4	2.12 (Ca,Sr)	0.24	0.36	0.36	0.04	-
19	3.5 (Ca,Y)	0.32	0.34	0.33	-	<0.01
6	0.8 (Ca,Y,Sr)	0.85	0.13	0.01	<0.1	<0.01

Thicknesses varied from less than 0.5 microns to over 3.0 microns. Most of the coatings contained roughly equimolar concentrations of the primary Ca-Ge-S constituents. However the coatings can be very air sensitive, resulting in the formation of  $\text{Ca(OH)}_2$  either at the air-coating interface or at the coating-anode interface. In the former case  $\text{Ca}^{++}$  ions are presumably transported through the film where they can react with moisture at the air interface. The thus transported Ca gives a  $\text{Ca(OH)}_2$  coating on top of the synthetic SEI, raising the apparent Ca concentration in the film above its true level; this effect is observed in Sample #6. In the future it will be essential to exercise greater caution in transferring these samples into the SEM chamber to avoid exposure to moisture and the related artifacts so produced.

Note that the concentration of the substituent cations,  $\text{Sr}^{++}$  and  $\text{Y}^{+3}$ , range from less than 1% (the detection limit) up to 4% in

the case of  $\text{Sr}^{++}$  in Sample #4. The  $\text{Ca}(\text{OH})_2$  coating on Sample # 6 (estimated to be about 7000 Angstroms thick) reduced the signal from the cation substituents by a factor of roughly 3, thereby rendering the  $\text{Sr}^{++}$  concentration essentially undetectable even if its level approached that of  $\text{Sr}^{++}$  in Sample #4.

#### 2.2.2. Film Morphology and Evidence for Ca Corrosion.

Figures 1 and 2 show the surface of Sample #1, a scraped but uncoated Ca anode at 1000X and 5100 X magnification. The grooves from scraping are evident in both views. The lighter mounds are clusters of  $\text{Ca}(\text{OH})_2$  particles which have nucleated and grown at discrete points on the Ca anode surface. Presumably the entire surface of the anode is coated by a surface layer of calcium hydroxide which has, for a time, some passivating capability. But, once this protective coating is breached, corrosion in air proceeds rapidly at the breached points, forming copious quantities of calcium hydroxide.

Figures 3 and 4 show the surface of Sample #2, a scraped Ca anode sputter coated with the basic Ca-Ge-S ternary composition with a thickness of 0.4 microns, at 500X and 5000X magnification. Figure 3 clearly shows the same calcium hydroxide clusters as in Sample #1 shown in Figures 1 and 2, except they occur beneath the sputtered coating as can be seen by a careful examination of Figure 3. The cause of this complete lack of passivation is evident in Figure 4, which shows the granular morphology of the coating, possibly but not necessarily associated with crystallites, whose

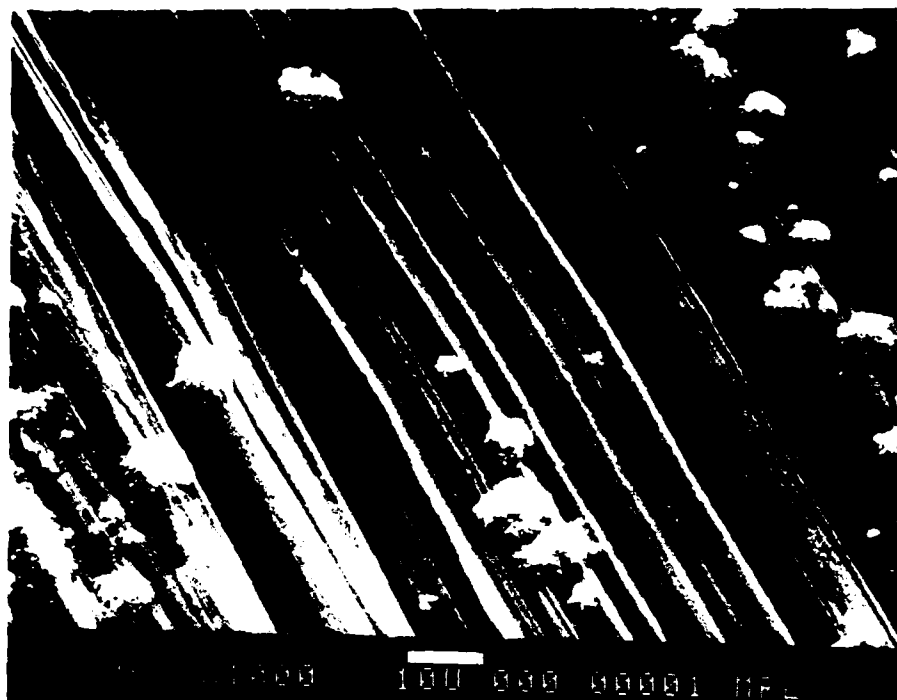


FIGURE 1, SAMPLE #1, SEM micrograph of scraped but uncoated Ca anode after some air exposure, 1000X.



FIGURE 2, SAMPLE # 1, 5100X.

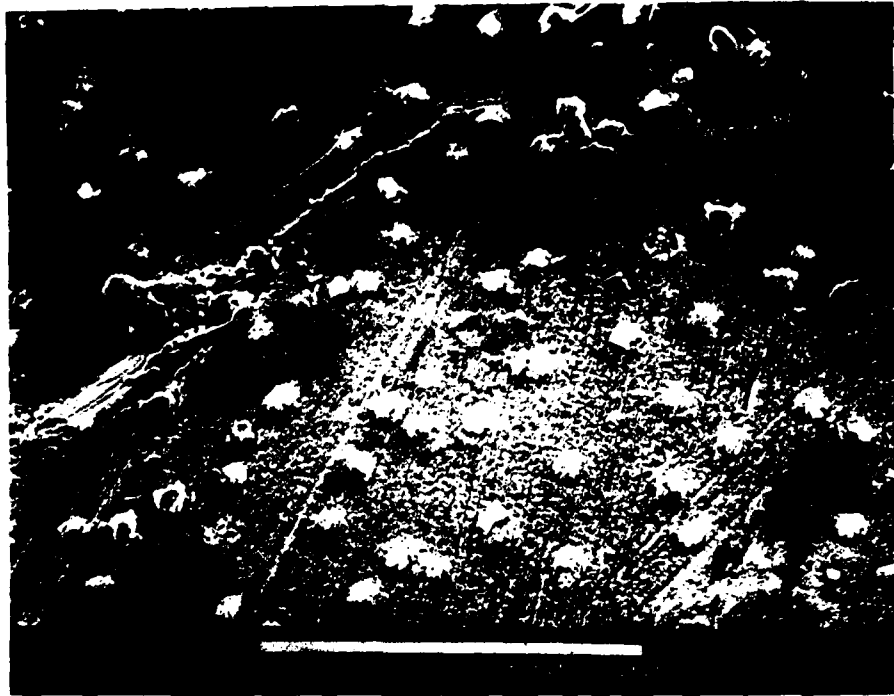


FIGURE 3, SAMPLE #2, SEM micrograph of sputtered Ca-Ge-S coating, 0.44 microns thick, on scraped Ca anode after some air exposure; 500X.

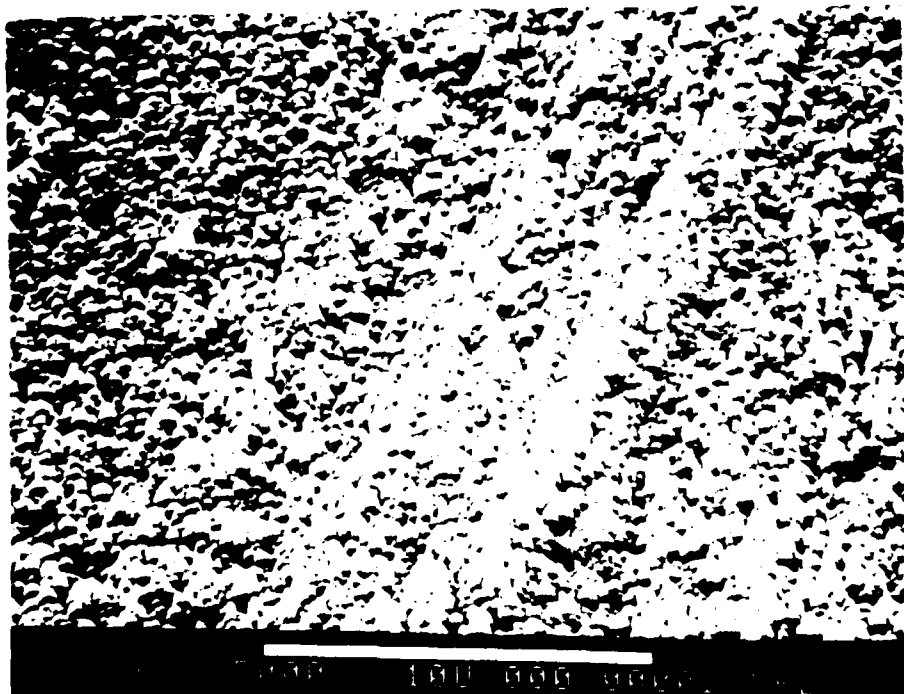


FIGURE 4, SAMPLE # 2, 5000X

scale has roughly the same dimension as the film thickness. Clearly the film must grow to a greater thickness for these grains to grow fully together and provide a completely protective coating.

The effect of greater film thickness is shown in Figures 5 and 6, 6000X and 5000X magnification views of the surface of Sample #19, a scraped Ca anode with a 3.5 microns thick coating of a Ca-Ge-S-Y quaternary composition. Note first the deep grooves scraped onto the bare anode are replicated by the surface of the coating as shown best in Figure 5 taken with the e-beam at a 43 degree angle of incidence. Superimposed on these grooves is a subtle granularity which is evidently associated with a columnar film morphology as shown in Figure 6, taken at an 83 degree tilt angle. The scale of this columnar structure is in the range of 0.1 - 0.2 microns, smaller than that of Sample #2. Note further that there is no evidence of calcium hydroxide at the coating-anode interface, verifying the compactness of the coating, or at the coating-air interface.

Finally we present morphological evidence from Sample #6, as shown in Figures 7 and 8 at 100X and 5000X magnification, respectively. This is the quinary Ca-Sr-Y-Ge-S sample which has already been discussed in Section 2.2.1, for which EDS evidence indicated the presence of calcium hydroxide at the coating-air interface. The surface morphology confirms this interpretation and suggests the presence both of a continuous hydroxide layer - evidenced by the faint lace-like structure caused by outgassing of a hydrated

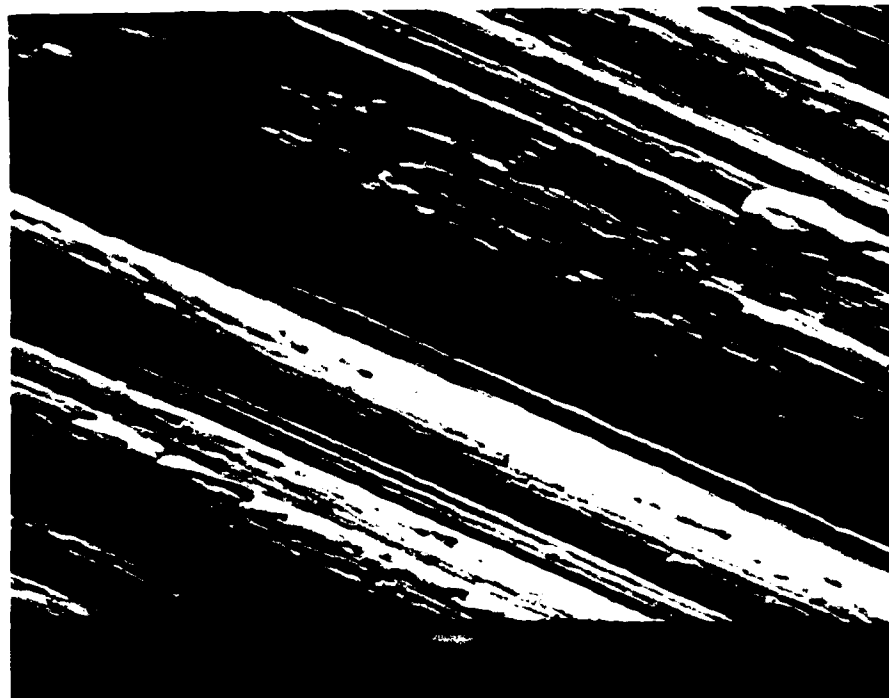


FIGURE 5, SAMPLE #19, Sputtered Ca-Y-Ge-S film, 3.5 microns thick, on scraped Ca anode after some air exposure; 6000X, 43° tilt.

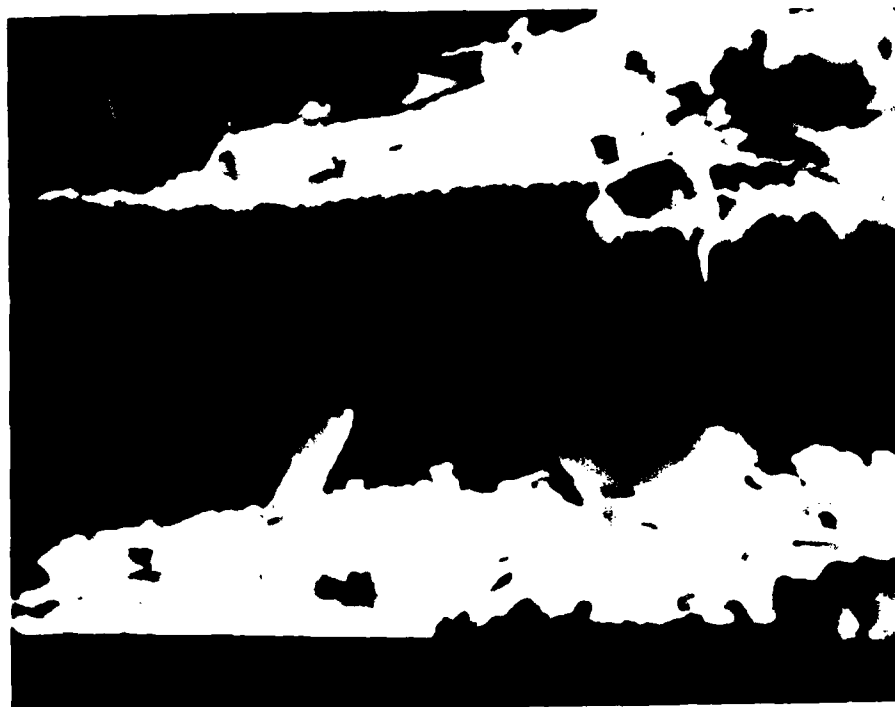


FIGURE 6, SAMPLE # 19, 6000X, 83° tilt.

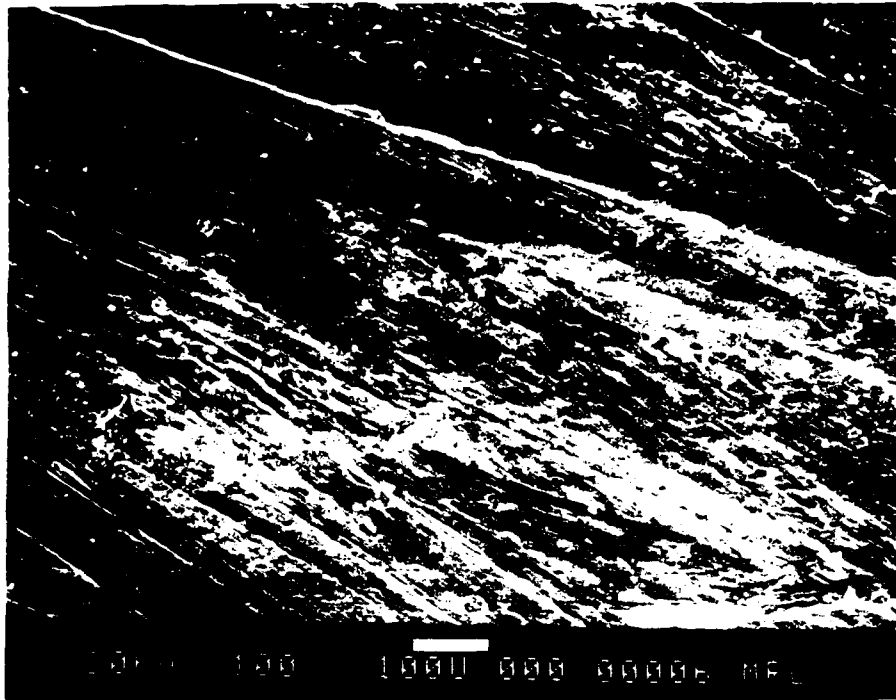


FIGURE 7, SAMPLE #6, Sputtered Ca-Y-Sr-Ge-S coating, 0.8 microns thick, on scraped Ca anode after some air exposure; 100X.

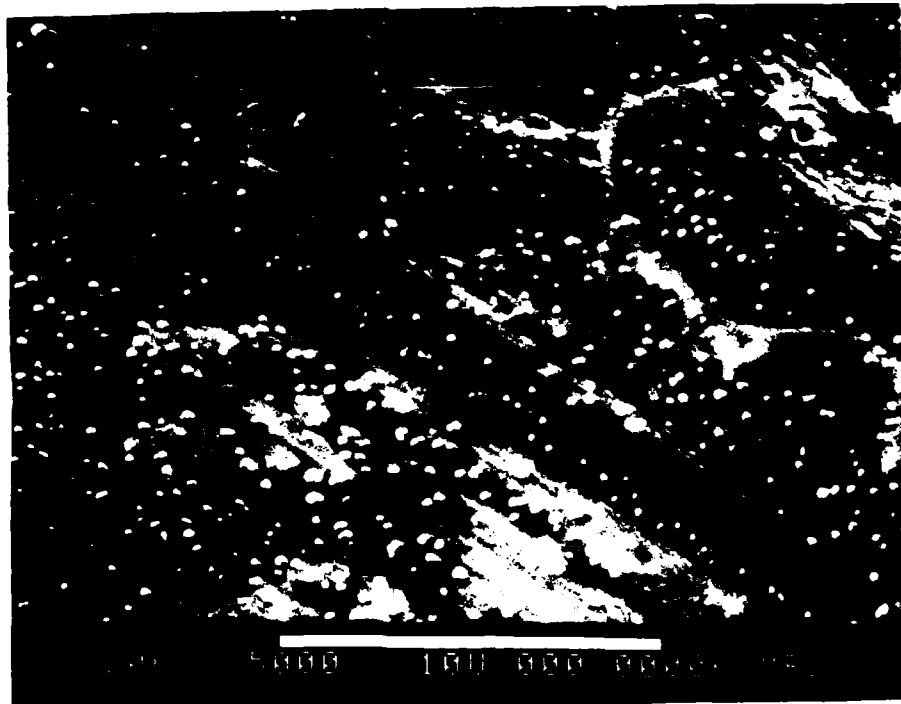


FIGURE 8, SAMPLE # 6, 5000X.

surface coating during pump-down to prepare the sample for SEM observation - and of individual Ca hydroxide crystallites or clusters of tiny crystallites - evidenced by the now familiar white mounds on the surface. These crystallites or clusters are of order 0.2 microns in size, far too small to detect unless they occurred at the free surface. Thus Ca ions successfully migrated through the protective coating to react with moisture at the free surface, evidence that the SSEI is effective in transporting  $\text{Ca}^{++}$  ions.

### 2.3 Conclusions

We conclude from these observations of uncoated and coated Ca anodes that a balance is required to assure that the coating is thick enough to be continuous and therefore passivating, yet thin enough to minimize its ohmic losses. Apparently the presence of additives contributes favorably to this balance, since the scale of surface granularity or columnar spacing is reduced by the addition of Y and Sr. There is no evidence for crystallinity in any of these films, although the coarser granularity in the ternary films causes strong scattering and absorption of incident light, rendering the coating black in reflection, compared to the reddish cast of the quaternary and quinary coatings.

## 3. TESTING OF BEAKER CELLS

### 3.1 Experimental

The coated electrodes were initially evaluated by testing in "beaker cells". These cells were constructed by placing the coated or reference uncoated Ca electrodes ( $3.2 \text{ cm}^2$  area) in a glass jar with a carbon counter electrode and the 1 molar  $\text{Ca}(\text{AlCl}_4)_2\text{-SOCl}_2$  catholyte. The electrodes were held at a separation of about 0.8 cm under flooded electrolyte conditions. This configuration introduces a voltage drop of about 0.78 V at our standard test current density of  $6.56 \text{ mA/cm}^2$ , far greater than the ohmic loss associated with the specific impedance in a conventional starved electrolyte cell configuration. However this configuration has the advantage that the anode can be easily removed and examined after discharge without mechanically disturbing the surface morphology.

As for the 1 M  $\text{Ca}(\text{AlCl}_4)_2\text{-SOCl}_2$  catholyte, we prepared several batches by dissolving thoroughly vacuum dried  $\text{CaCl}_2$  (Aldrich) in the appropriate concentration of  $\text{Al}_2\text{Cl}_6$  (Witco) in  $\text{SOCl}_2$  (Mobay). For the hermetically sealed cells we purchased one liter of the same catholyte from Anderson Physics Laboratories. This batch was completely clear in appearance, whereas ours was slightly cloudy. However the cell impedance was about 30% higher for cells assembled with the Anderson electrolyte, suggesting the possibility that the salt concentration might have been somewhat lower than for our own material.

Cells were assembled, filled with  $\text{Ca}(\text{AlCl}_4)_2\text{-SOCl}_2$  catholyte, stored for two days at room temperature, and discharged at constant current while monitoring the discharge voltage. The par-

tially discharged cells were then stored for several weeks or more at room temperature before being disassembled for further SEM and EDS evaluation.

### 3.2 Results and Discussion

#### 3.2.1 Electrochemical Testing

A number of reference cells using calcium anodes and carbon cathodes in a glass cell, as described above, were assembled and tested. These cells were tested at 6.5 and 12.6 mA/cm<sup>2</sup> rates after various durations of storage at room temperature. Cells stored for more than two days and discharged particularly at 12.6 mA/cm<sup>2</sup> rate showed voltage fluctuations in the initial discharge. Therefore to evaluate the Ca<sup>++</sup> ionic conduction of the SEI coatings, a standard test discharge at a 6.5 mA/cm<sup>2</sup> after two days storage at room temperature was selected. A typical initial discharge of a reference cell stored for two days at room temperature and discharged at 6.5 mA/cm<sup>2</sup> current density is shown in Fig. 9. Our designed cell configuration introduces a voltage drop of about 0.78 V at 6.5 mA/cm<sup>2</sup> drain due to electrolyte impedance. The electrolyte conductivity calculated from this impedance is about  $6.7 \times 10^{-3} \text{ ohm}^{-1} \text{ cm}^{-1}$ .

Four cells were made in a similar way with the calcium electrodes coated with binary films of Ge-S. Two of these coated electrodes were annealed for 30 hours to introduce calcium by diffusion prior to their use in the cells. All of these cells failed during

# VOLTAIX INC

INITIAL DISCHARGE AT 6.5mA/cm squared

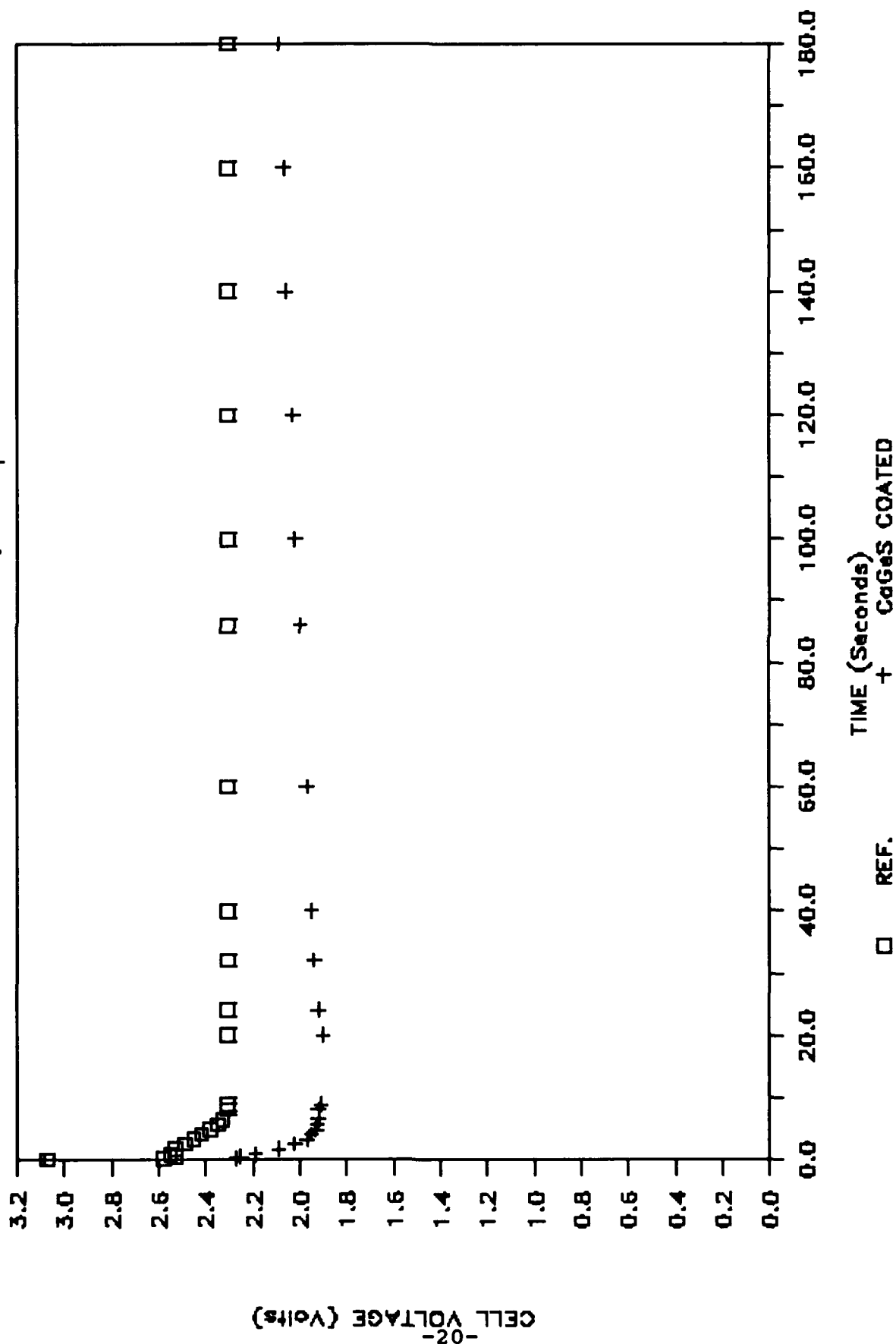


FIGURE 9. Discharge data for reference and ternary coated anodes.

standard discharge indicating that the SEI binary coatings are impervious to  $\text{Ca}^{++}$  ion conduction.

Calcium electrodes with ternary SEI coatings were made by cosputtering calcium and germanium in a 5%  $\text{H}_2\text{S}/\text{Ar}$  plasma. The coatings so formed had the approximate stoichiometry  $\text{Ca}_{.33}\text{Ge}_{.33}\text{S}_{.33}$ . Calcium electrodes with ternary SSEI coatings of 0.2, 0.4 and 0.87 microns thickness were made in three different runs. Cells were assembled using coated electrodes from each run, stored for two days at room temperature and tested at  $6.5 \text{ mA}/\text{cm}^2$ . The cells showed open circuit voltages similar to the reference cells (3.08 V - 3.10 V). A characteristic discharge of the ternary coated calcium anode cells is compared with the reference cell discharge in Fig. 9. The running voltage of the coated Ca anode cell was 2.05 V vs. 2.30 V for the reference. The results show that the ternary coating conducts  $\text{Ca}^{++}$  ions, otherwise no current could be drawn through the coating. Secondly, the coating retains its adherence on the calcium substrate, at least during initial discharge, otherwise there would be a voltage delay followed by a rise in voltage to a typical running voltage for an uncoated Ca reference cell. The presence of the coating on the electrodes after discharge was verified visually. Each cell was then stored for three weeks before its anode was removed for SEM/EDS observation, which confirmed the continued presence of the coating.

From the coating impedance of 0.25 V observed in the discharge at  $6.5 \text{ mA}/\text{cm}^2$ , and the thickness of the coating (0.43 microns in the above example), the ionic conductivity of the SSEI was calculated

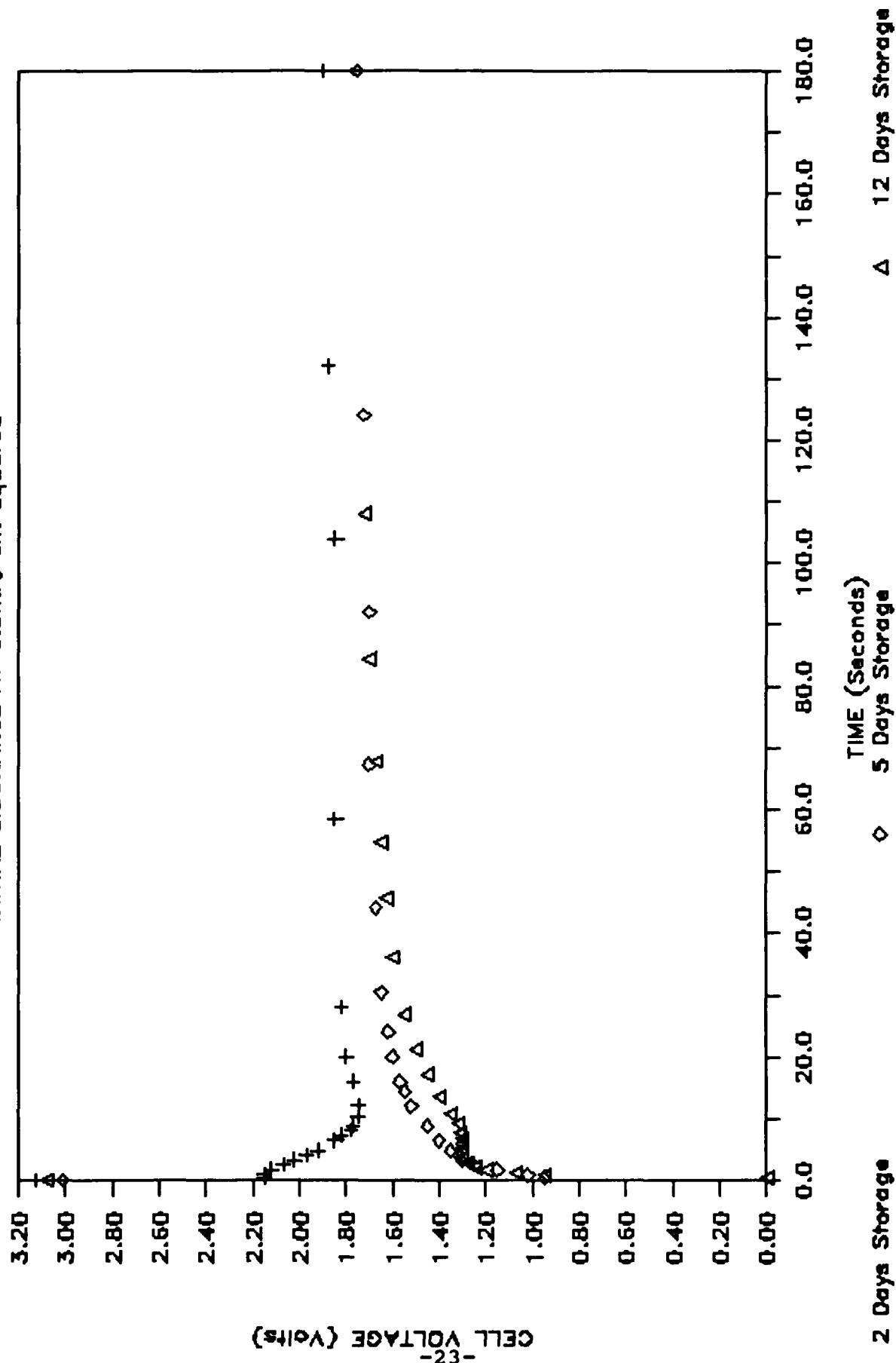
to be  $1.1 \times 10^{-6} \text{ ohm}^{-1}\text{cm}^{-1}$ . The data on three coated Ca anode cells indicate that the ionic conductivity of the ternary SSEI coatings is in the range  $1.1 \times 10^{-6}$  to  $2.4 \times 10^{-7} \text{ ohm}^{-1}\text{cm}^{-1}$ .

The effects of doping these films with  $\text{Sr}^{++}$  or  $\text{Y}^{+3}$  ions on the  $\text{Ca}^{++}$  ionic conductivity was studied by electrochemical discharge of cells having anodes coated with quaternary films. Such coatings were prepared in the same manner as the ternary coatings except that additional coupons of Sr metal or Y metal were affixed on the composite Ca + Ge sputtering target. Calcium electrodes were coated with  $\text{Sr}^{++}$  doped quaternary films of 0.69 microns to 2.7 microns in four separate runs. Electrodes coated with 0.69 and 2.12 microns were used in the cells. A 1 M  $\text{Ca}(\text{AlCl}_4)_2\text{-SOCl}_2$  catholyte obtained from Anderson Physics Laboratories was used for cell testing. To evaluate the differences in the electrolytes, two reference cells with uncoated and scrapped calcium anodes were assembled and tested after two days storage at room temperature. The discharge curves for the new electrolyte at  $6.5 \text{ mA/cm}^2$  current density and after 2, 5, and 12 days storage at room temperature are shown in Fig. 10. The new electrolyte introduces a voltage drop of 1.22 V compared to 0.78 V with our electrolyte at  $6.5 \text{ mA/cm}^2$ . From the observed electrolyte impedance, the ionic conductivity of the new Anderson Physics Laboratory electrolyte is calculated to be  $4.30 \times 10^{-3} \text{ ohm}^{-1}\text{cm}^{-1}$ , somewhat lower than the conductivity of our electrolyte ( $6.7 \times 10^{-3} \text{ ohm}^{-1}\text{cm}^{-1}$ ), but in the same range as that reported for 1 M  $\text{Ca}(\text{AlCl}_4)_2\text{-SOCl}_2$  catholyte by Saft<sup>5</sup>.

# VOLTAIX INC

INITIAL DISCHARGE AT 6.5mA/cm squared

FIGURE 10. Discharge data for reference Ca in A.P.L. electrolyte.



A characteristic discharge of a  $\text{Sr}^{++}$  substituted quaternary SSEI coated Ca anode cell is compared with the reference cell in Fig. 11. From the voltage drops due to the coating impedances, ionic conductivities of the coatings were calculated for the two cells to be  $2.4 \times 10^{-6}$  and  $5.4 \times 10^{-6} \text{ ohm}^{-1} \text{ cm}^{-1}$ .

The calcium electrodes coated with 1.6 and 2.1 microns thick  $\text{Y}^{+3}$  doped quaternary films were assembled in cells and tested. The discharge of the cell with the 1.6 micron anode coating compared with the reference cell is shown in Fig. 12. A voltage drop of 0.065 V due to the coating impedance is observed at the  $6.56 \text{ mA/cm}^2$  rate. The ionic conductivity of this coating, calculated from the observed impedance, is about  $1.6 \times 10^{-5} \text{ ohm}^{-1} \text{ cm}^{-1}$ , as compared to an ionic conductivity of  $3.2 \times 10^{-6} \text{ ohm}^{-1} \text{ cm}^{-1}$  for the anode with the 2.1 micron quaternary coating.

Finally, the quinary (Ca-Ge-S) films as doped with  $\text{Sr}^{++}$  plus  $\text{Y}^{+3}$  were prepared in a similar way except that additional coupons of Sr metal and Y metal were affixed onto the composite Ca + Ge sputtering target. Coatings of 0.8 to 2.2 microns on calcium electrodes were obtained in three different runs. Two cells were made and tested after 2 days storage at room temperature. From the observed coating impedances, the ionic conductivities of the quinary SSEI's were calculated to be  $2.3 \times 10^{-6}$  and  $8.8 \times 10^{-7} \text{ ohm}^{-1} \text{ cm}^{-1}$ .

# VOLTAIX INC

INITIAL DISCHARGE AT 6.5mA/cm squared

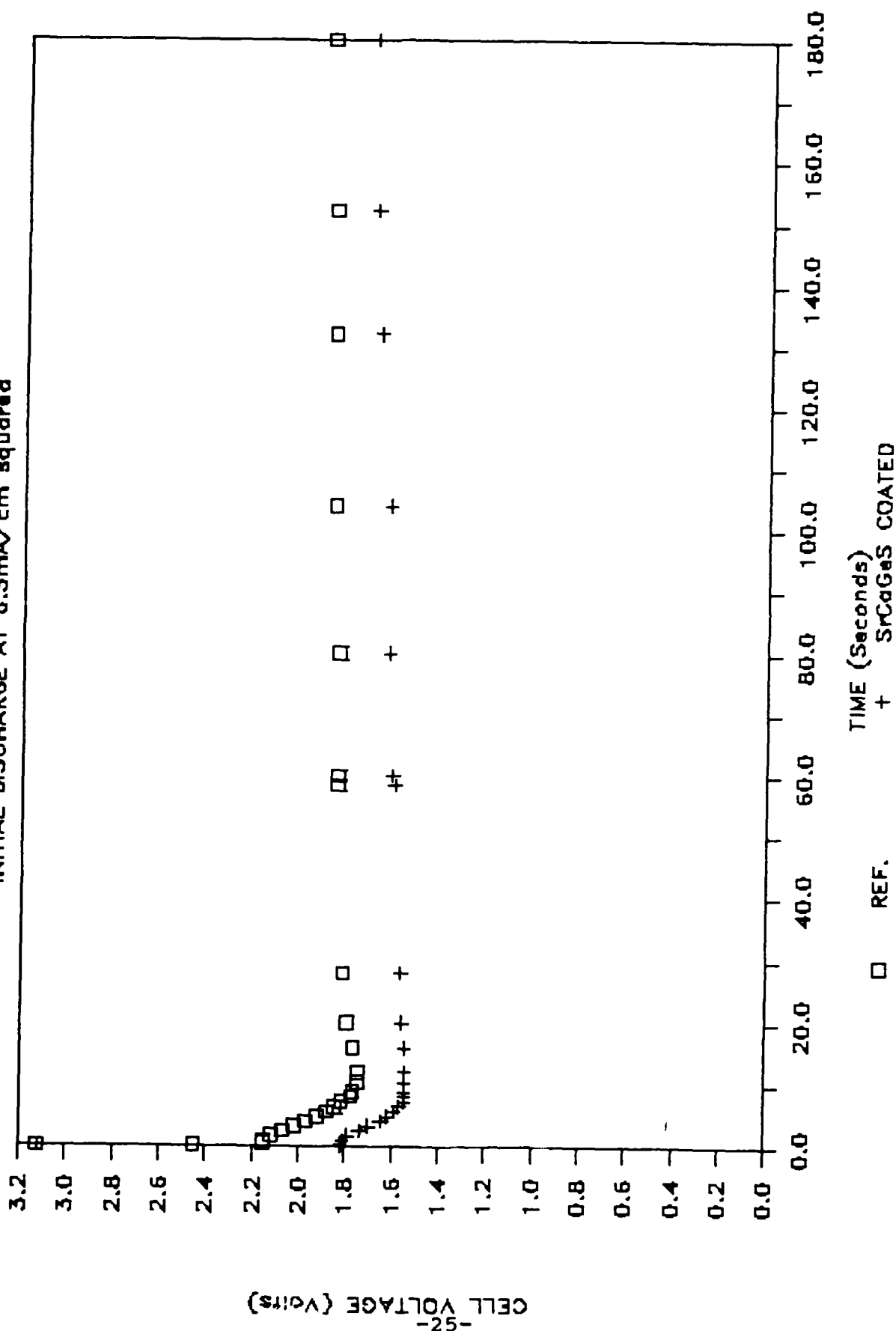
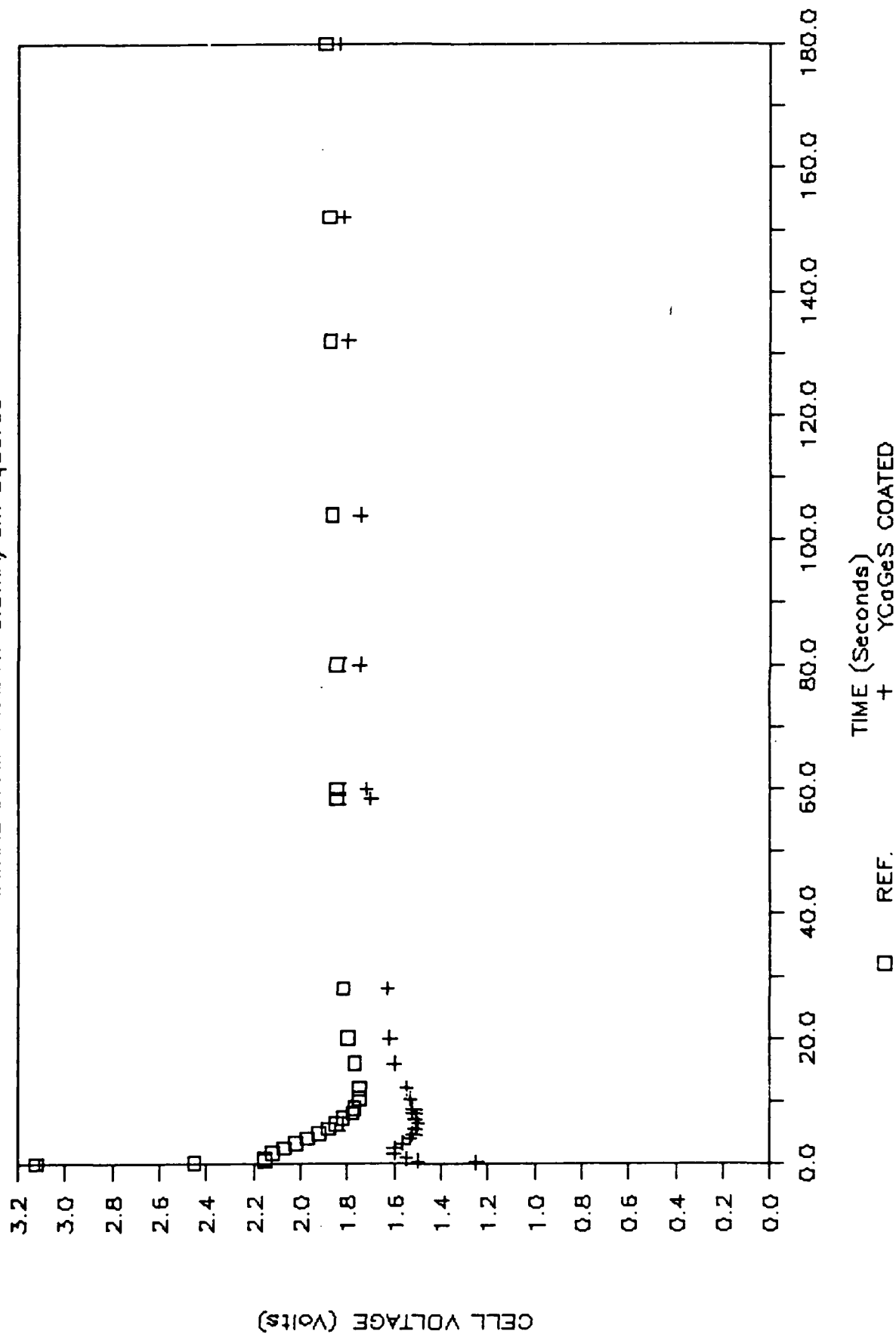


FIGURE 11. Discharge of a Ca-Sr-Ge-S coated anode vs. reference.

VOLTAIX INC  
INITIAL DISCHARGE AT 6.5mA/cm squared

FIGURE 12. Discharge of a Ca-Y-Ge-S coated anode vs. reference.



The ionic conductivities of the ternary and the  $\text{Sr}^{++}$  and/or  $\text{Y}^{+3}$  doped SSEI coatings are tabulated below:

TABLE 2 -  $\text{Ca}^{++}$  Ionic Conductivities of SSEI Coatings.

Substituent Ion	Calculated Ionic Conductivity, $\text{ohm}^{-1}\text{cm}^{-1}$
$\text{Ca}^{++}$ (base case)	$2.4 \times 10^{-7}$ - $1.1 \times 10^{-6}$ (3 data points)
$\text{Sr}^{++}$	$2.4 \times 10^{-6}$ - $5.4 \times 10^{-6}$ (2 data points)
$\text{Y}^{+++}$	$3.2 \times 10^{-6}$ - $1.6 \times 10^{-5}$ (2 data points)
$\text{Y}^{+++} + \text{Sr}^{++}$	$8.8 \times 10^{-7}$ - $2.3 \times 10^{-6}$ (2 data points)

Clearly the substitution of  $\text{Y}^{+3}$  for  $\text{Ca}^{++}$ , even in low concentrations, appears to enhance the  $\text{Ca}^{++}$  ion conduction more effectively than does the  $\text{Sr}^{++}$  substitution. The  $\text{Y}^{+3}$  doped coatings are comparatively more compact, thus providing improved calcium corrosion protection as well. Further optimization with  $\text{Y}^{+3}$  doping to increase the ionic conductivity could make the  $\text{Ca-SOCl}_2$  cells of commercial value. Recently Peled<sup>7</sup> has reported improvements in corrosion and low temperature characteristics of  $\text{Ca-SOCl}_2$  cells with  $\text{Sr}(\text{AlCl}_4)_2$  electrolytes. However the ionic conductivity of the SEI in  $\text{Sr}(\text{AlCl}_4)_2$  and  $\text{Ca}(\text{AlCl}_4)_2$  was found to be the same.

### 3.2.2 Anode Morphology and Surface Chemistry - EDS and SEM - Observations.

After the completion of electrochemical testing and storage of the cells for two to four weeks, several cells were disassembled for SEM observation and EDS surface chemical analysis. The coated and uncoated reference Ca anodes were thoroughly rinsed in pure  $\text{SOCl}_2$  and allowed to dry under argon atmosphere. The anodes were

then transferred to the SEM in air and subjected to EDS analysis. Typical results are listed in Table 3.

TABLE 3 - EDS Analysis of Discharged Electrodes.

Sample #	Thickness, microns; (cation(s))	Relative EDS Signal						
		Ca	Cl	Al	S	Ge	Sr	Y
12	(none)	0.24	0.72	0.04	-	-	-	-
13	0.69 (Ca, Sr)	0.13	0.51	0.13	0.207	0.03	<0.01	-
14	2.12 (Ca, Sr)	0.21	0.68	<0.01	0.10	0.01	<0.01	-
15	0.8 (Ca, Sr, Y)	.27	0.47	<0.01	0.22	0.04	<0.01	<0.01
16	2.2 (Ca, Sr, Y)	.29	0.50	<0.01	0.06	0.15	<0.01	<0.01

The surface of Sample #12 was enriched in chlorine, with only a trace of aluminum, suggesting that the free surface layer is nearly pure  $\text{CaCl}_2$ , with a trace of the  $\text{Ca}(\text{AlCl}_4)_2$  salt but no thionyl chloride solvent remaining. The  $\text{CaCl}_2$  is extremely hygroscopic, forming an aqueous surface phase when exposed to air prior to the vacuum coating of the SEM sample. This hydrate then outgassed moisture during sample metalization, as can be visualized by observing the bubbles on the sample surface as shown in Figure 14, a 100X SEM image of this sample. The surface was extremely irregular, indicating substantial Ca corrosion accompanying formation of the  $\text{CaCl}_2$  passivation layer. The coated films also had considerable  $\text{CaCl}_2$  on their surface, but all retained some chemical indication of the presence of the SSEI film as evidenced by the S and Ge EDS signals in Samples #13, 14



FIGURE 13, SAMPLE #12, SEM Micrograph of discharged calcium electrode, 100X.

15 and 16. Sample #16, in particular, had a relatively high level of Ge indicating that the  $\text{CaCl}_2$  coating had an average thickness of less than about 0.3 microns, otherwise the Ge L-alpha x-ray signal would be totally absorbed. Thus there is direct chemical evidence that the SSEI coatings, insoluble in the catholyte, remain in place both during and after discharge, and reduce the corrosion of the Ca anode by the catholyte, as evidenced by reduced  $\text{CaCl}_2$  formation.

The morphology of typical coated anodes after discharge is shown in Figures 14 and 15 showing Samples #15 and 16, respectively, at 500X magnification. The crusty deposit in Figure 14 is a thin layer of  $\text{CaCl}_2$ , slightly cracked and bulged by interactions with atmospheric  $\text{H}_2\text{O}$  during sample preparation, uniformly coating the SSEI. It is estimated from the L-alpha x-ray signal of the Ge from this sample (see Table 2) that the  $\text{CaCl}_2$  coating has an approximate thickness of 0.7 microns.

In Figure 15, however, only the smooth Ca-Sr-Y-Ge-S SSEI coating is seen, breached at scattered points by pits of corrosion. This Ca anode had been scraped prior to coating deposition, but the Ca thickness variations so produced were apparently smoothed out during discharge and the SSEI layer was flexible enough to conform itself to the new Ca surface morphology. This is our best example of a SSEI coating after cell discharge, and clearly indicates that the SSEI coatings can both reduce corrosion and permit  $\text{Ca}^{++}$  ion transport at a sufficient rate to permit the coating to remain intact during discharge.

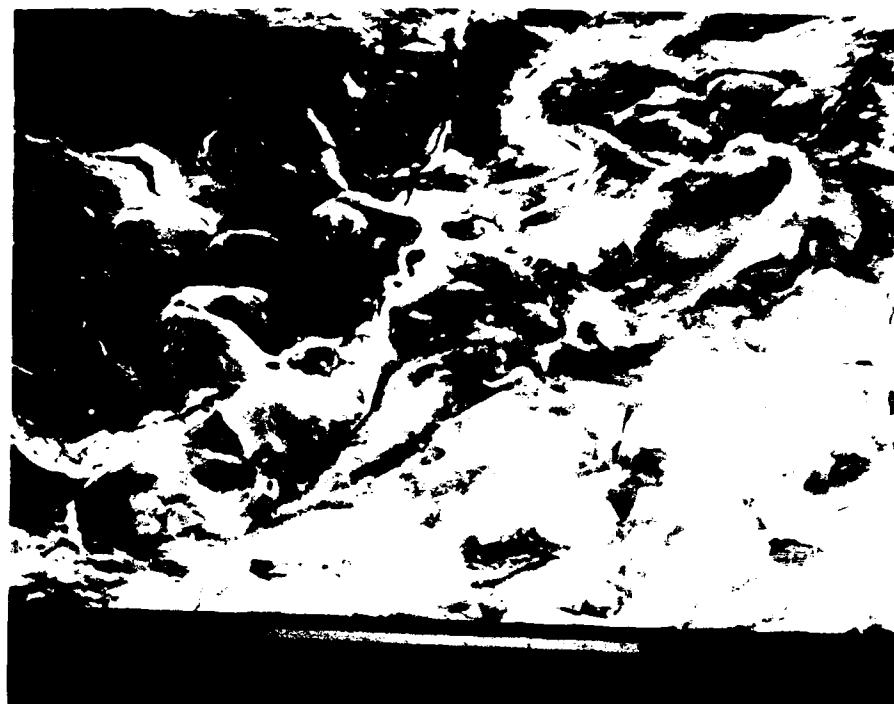


FIGURE 14, SAMPLE #15, SEM micrograph of discharged Ca-Sr-Y-Ge-S coated electrode, 0.8 microns thick, 500X.

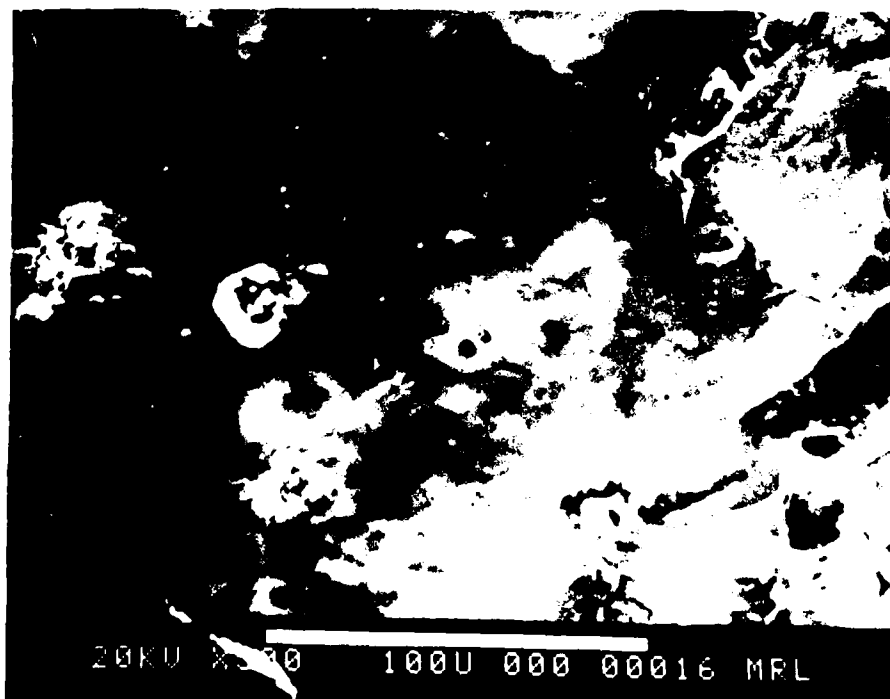


FIGURE #15, SAMPLE #16, SEM micrograph of discharged Ca-Sr-Y-Ge-S coated electrode, 2.2 microns thick, 500X.

### 3.3 Conclusions.

The electrochemical discharge data have shown that ternary, quaternary and quinary sputter coatings based on the Ca-Ge-S system with additives of  $\text{Sr}^{++}$  and/or  $\text{Y}^{+3}$  have  $\text{Ca}^{++}$  ionic conductivities in the range  $10^{-5}$  to  $10^{-7} \text{ ohm}^{-1}\text{cm}^{-1}$ . These SSEI coating on calcium stay intact during partial discharge. SEM and EDS surface analysis data show a heavy overlayer of  $\text{CaCl}_2$  on uncoated calcium electrodes whereas only extremely thin (0.3 to 0.7 micron) deposits of  $\text{CaCl}_2$  are observed on the coated anodes. The SEM and surface elemental analysis of the partially discharged electrodes confirm the integrity of the SSEI on coated electrodes both during and after discharge.

### 4. SUMMARY.

The main conclusions from the Phase I project relate to the demonstration that RF sputtered coatings based on the Ca(Sr,Y)-Ge-S system can serve as an effective SSEI for Ca anodes in Ca- $\text{SOCl}_2$  primary cells using 1 M  $\text{Ca}(\text{AlCl}_4)_2$  as the electrolyte. Thus we have shown that such films, in thicknesses ranging between 0.8 to 3.5 microns, are insoluble in this catholyte system at  $21^\circ\text{C}$ , are good  $\text{Ca}^{++}$  ionic conductors in the range  $10^{-5}$  to  $10^{-7} \text{ ohms}^{-1} \text{ cm}^{-1}$ , and can protect Ca from the corrosive effects of this electrolyte at  $21^\circ\text{C}$ .

More research, proposed to be performed under a Phase II program, will be necessary to show that these coatings can function as an

effective SSEI over the whole range of temperatures of interest for Army applications. Remaining to be demonstrated are the following points:

1. That these coatings are insoluble in the  $\text{Ca}(\text{AlCl}_4)_2\text{-SOCl}_2$  catholyte, possibly with  $\text{SO}_2$  addition, up to  $70^\circ\text{C}$ .
2. That the  $\text{Ca}^{++}$  ionic conductivity of these SSEI's is high enough at low temperatures to make such coatings useful over the entire range of required discharge rates and operating temperatures.
3. That the coatings are, or can be made to be, sufficiently tough to resist delamination from the Ca anode foil during the winding of coated Ca anodes for high rate jelly-roll  $\text{Ca-SOCl}_2$  cells.
4. That the corrosion inhibition properties of these SSEI coatings can make a dramatic contribution to reducing the rate of Ca corrosion and thus the maintainance of  $\text{Ca-SOCl}_2$  cell capacity after storage for extensive time at  $70^\circ\text{C}$ .

## 5. REFERENCES

1. E. Peled, 32nd Power Sources Symposium, 1986.
2. C. W. Walker, Jr., W. L. Wade, Jr., M. Binder and S. Gilman, J. Electrochem. Soc., 133, 1555 (1986).
3. R. J. Staniewicz, S. Hafner and R. A. Dixon, Second Quarterly Report, SLCET-TR-86-0013-2 (Jan. 1987).
4. W. K. Behl, U.S. Patent 4474863.
5. R. J. Staniewicz, S. Hafner and R. A. Dixon, Third & Fourth Quarterly Report, SLCET-TR-86-0013-4 (May & July 1987).
6. C. Walker, Jr. and M. Binder, 33rd Power Source Symposium, (June 1988).
7. E. Peled, 33rd Power Source Symposium, (June 1988).
8. D. S. Rajoria and J. P. de Neufville, Proc. 32nd Power Sources Symposium, 488 (1986).